INTERNATIONAL JOURNAL OF AUTOMOTIVE SCIENCE AND TECHNOLOGY

2025, VOL. 9, NO:4, 527-535 www.ijastech.org e-ISSN: 2587-0963

Enhancement of Ride Comfort in Active Quarter-Car Suspension Systems using Model Predictive Control

Duc Lich Luu[1]*, Nguyen Quang Trung[1], Ngoc Thien To[2]

[1]*Faculty of Transportation Mechanical Engineering, the University of Danang - University of Science and Technology, 54 Nguyen Luong Bang, 550000, Da Nang, Vietnam.*
[2]*Faculty of Mechanical - Automotive and Civil Engineering, Electric power university, 235 Hoang Quoc Viet, 100000, Ha Noi, Vietnam.*

Research Article

Abstract

In recent years, the use of active suspension systems in passenger cars has gained significant attention due to their ability to enhance ride comfort. These systems are designed to automatically adjust the control force, adapting to different driving conditions and the varying forces caused by road surface irregularities. This paper explores the implementation of the Model Predictive Control (MPC) algorithm for managing an active suspension system modeled by a quarter-car vibration model in the longitudinal direction. Simulations were performed using Matlab/Simulink to compare the performance of the MPC-controlled system with those governed by a PID controller and a conventional passive suspension system. Simulation results highlight that the MPC controller provides significant improvements in multiple aspects of suspension performance. Specifically, it achieves a noticeable reduction in body acceleration, ensuring smoother ride comfort for passengers. Moreover, the MPC-based suspension maintains lower body displacement and more stable suspension deflection, which translates into improved vehicle handling and road holding. Compared to PID and passive configurations, the MPC approach shows a faster adaptation to varying road profiles and more efficient suppression of vibrations across sinusoidal, step, and random road excitations. These outcomes emphasize the superiority of MPC in balancing ride comfort, safety, and vehicle stability, confirming its potential as an effective control strategy for future suspension systems.

Keywords: Automotive Dynamics; Suspension System; Active Suspension System; Ride Comfort;

History
Received 19.05.2025
Revised 16.08.2025
Accepted 24.09.2025

Contact
* Corresponding author:
Duc Lich Luu,
ldlich@dut.udn.vn
Address: University of Danang - University of Science and Technology, Da Nang, Vietnam.
Tel: (+84.236) 3736945/

To cite this paper: Luu, D.L., Trung, N.Q., To, N.T. Enhancement of Ride Comfort in Active Quarter-Car Suspension Systems using Model Predictive Control. International Journal of Automotive Science and Technology. 2025; 9 (4): 527-535. http://dx.doi.org/10.30939/ijastech..1701968

1. Introduction

The suspension system in cars is a crucial component in the mechanical structure of the car. It plays a keyyrole in ensuring the movement of the entire car chassis, affecting the driving experience and passenger comfort. A car is a complex oscillating system, closely linked to the roaddsurface. The vibrations of the car not only impact the passengers and cargo being transported, but also affect the durability of the car's structural components, as well as negatively influence the driving experience of the driver. Therefore, suspension systems are developed to address issues related to ride comfort and safety in car movement [1]. In the case of using a passive suspension system, it can respond to various road surfaces with different levels of roughness, but there remains a conflict between the damping coefficient and factors concerning safety and ride comfort.

One idea applied to improve the vibrations of cars is the use of active suspension systems to meet the requirements of ride comfort and safety when traveling on all types of roads. The characteristics of this suspension system are adjusted depending on the specific conditions of each type of road [2]. The active suspension system still includes the basic components of a conventional passive suspension system, but with the addition of a separate hydraulic actuator integrated at each position of the suspension system [3]. This enables the active suspension system to independently adjust and regulate the damping force and spring stiffness of each wheel, based on the road conditions and the specific driving mode. This approach helps optimize the suspension system's response to various road conditions, ensuring the car operates safely and comfortably on all types of terrain. Numerous studies have been conducted to address the behavior of actuators in response to various road profiles [4], [5].

One of the main development trends that major car manufacturers are currently focusing on is the design of active suspension systems [6]. Through the analysis of published works, many studies both domestically and internationally have emerged with the aim of proposing optimal control methods for

the system. In [6], the authors developed and implemented a sliding mode controller for a quarter-car model. The results showcase the superior performance and stability of the active suspension system in comparison to the passive suspension system. In [7], the authors employed a fuzzy controller to manage the active suspension system in cars. The results show that the fuzzy controller outperformed other methods. In [8], the authors utilized a fuzzy logic-based neural network to design the active suspension system. Meanwhile, in [9], two distinct controllers were developed for a quarter-car electric car modeluusing the LQR control method, aiming to improve both rideecomfort and safety, offering better performance compared to the passive suspension system. Other research employed the quarter-car model with various control strategies, including optimal control methods in [10], adaptive control in [11], and linear robust control in [12]. Research on controlling semi-active suspension systems has also been addressed using the quarter-car model, such as multi-objective control in [13].

The MPC algorithm, as introduced in [14], [15], is an advanced process control technique that effectively manages constraints by incorporating them during the design phase. A key benefit of the MPC approach is its ability to model both dynamic and static interactions between inputs, outputs, and disturbances, while systematically accounting for constraints on both inputs and outputs. However, much of the related literature applies MPC in combination with nonlinear formulations, heuristic optimization, or adaptive techniques. PID controllers, on the other hand, remain widely used in practice due to their simplicity, but they are often presented only as a baseline rather than being systematically compared to predictive strategies under a consistent framework. This gap motivates the present study, which focuses on the direct comparison of well-established PID and MPC methods for active suspension control. Both controllers are implemented on a quarter-car suspension model in MATLAB-SIMULINK, and their performance is evaluated relative to a passive suspension benchmark. By employing the same modeling environment and identical input conditions, the study provides a transparent and fair assessment of how each control approach influences vehicle ride comfort and stability.

The main contributions of this paper are as follows:

A systematic comparison of PID and MPC controllers for active suspension systems, ensuring a fair and transparent evaluation of both control strategies under identical conditions.

An evidence-based analysis showing that MPC achieves superior ride comfort and stability compared with PID and passive suspension.

A bridge between classical and modern perspectives, positioning MPC not only as an advanced method but also as a practically viable alternative for suspension design and implementation.

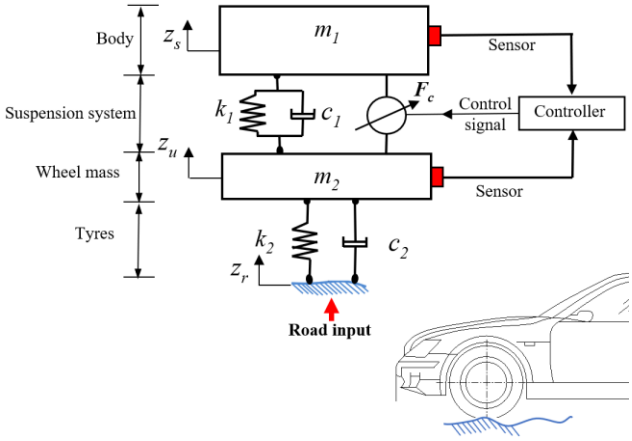

Figure.1. Car dynamic model

The remainder of the paper is organized as follows: Section 2 develops the research model for the suspension system. Section 3 presents the development of the algorithm for the controller. Section 4 analyzes the simulation results of the dynamics of the active suspension system. The final section discusses the conclusions and possible future research directions.

2. Mathematical Modeling

In this study, a quarter-car model of the passenger car suspension system is applied for research purposes. The car includes the body (sprung mass), suspension system, axle (unsprung mass), and tires. The basic components of the suspension system are illustrated as shown in Figure 1. Here, z_r represents the excitation signal from the road surface irregularities, while F_c is the control signal of the system. The specific parameters of the model have been presented in [16].

The principle of operation of the active suspension system is continuous monitoring of the distance between the car body and the suspension arms through ride height sensors. These sensors provide information about the car 's ground clearance, while speed sensors record and transmit the car speed signals to the suspension system controller. The task of the controller is to receive signals from the sensors and control the force and stiffnessoof the springs as well as the carhheight, depending on the operatinggconditions of the car. This is achieved through the control actuator system, which adjusts the damping force and stiffnessoof the suspension.

The electronic control actuator responds precisely to the continuous changes in the car's operating conditions, ensuring that the suspension system functions efficiently and provides comfort and safety for both passengers and the driver.

From Figure 1, applying the D'Alembert principle and newton's second law, the dynamiccequation of the car body is as in [9]:

$$m_1\ddot{z}_s + c_1\left(\dot{z}_s - \dot{z}_u\right) + k_1\left(z_s - z_u\right) = F_c. \quad (1)$$

Similarly, the dynamiccequation of the axle is as in [9]:

$$\begin{aligned} &m_2\ddot{z}_u - c_1(\dot{z}_s - \dot{z}_u) - k_1(z_s - z_u) \\ &+k_2(z_u - z_r) + c_2(\dot{z}_u - \dot{z}_r) = -F_c, \end{aligned} \tag{2}$$

where: m_1 is the sprunggmass; m_2 is the unsprunggmass; k_1, c_1 are the stiffness and damping coefficientsoof the suspension system; k_2, c_2 are the stiffness and damping coefficients of the tire system. The system has twoodegrees of freedom, represented by the vertical displacement of the car body and axle, z_s, z_u, corresponding to the body and axle displacements, and z_r is the height of the road surface irregularities. The force is generated by a hydraulic actuator F_c, and the actuator is capable of producing a force within the range $[F_c^{lower}, F_c^{upper}]$. It can be noted that if $F_c = 0$, Eq.(1) and Eq.(2) become the equations of the passive suspension system. Diagrams of controllers are shown in Figure 2 and Figure3.

Eq.(1) and Eq.(2) can be rewritten in the state-space form as follows:

$$\begin{aligned} \dot{\xi}(t) &= A_c\xi(t) + B_c u(t) \\ Y_{out}(t) &= C_c\xi(t). \end{aligned} \tag{3}$$

The state vector is defined as: $\xi = [z_s - z_u \;\; \dot{z}_s \;\; z_u - z_r \;\; \dot{z}_u]^T$, where the control input is $u = [\dot{z}_r \;\; F_c]$, with the following matrices: $A_c \subseteq \mathbb{R}^{4\times4}$, $B_c \subseteq \mathbb{R}^{4\times2}$, $C_c \subseteq \mathbb{R}^{4\times4}$:

$$A_c = \begin{bmatrix} 0 & 1 & 0 & -1 \\ -\frac{k_1}{m_1} & -\frac{c_1}{m_1} & 0 & \frac{c_1}{m_1} \\ 0 & 0 & 0 & 1 \\ \frac{k_1}{m_2} & \frac{c_1}{m_2} & \frac{k_1}{m_2} & -\frac{c_1+c_2}{m_2} \end{bmatrix}, \quad B_c = \begin{bmatrix} 0 & 0 \\ 0 & \frac{1}{m_1} \\ -1 & 0 \\ \frac{c_2}{m_2} & \frac{-1}{m_2} \end{bmatrix},$$

$$C_c = \begin{bmatrix} 1 & 0 & 0 & 0 \\ 0 & 1 & 0 & 0 \\ 0 & 0 & 1 & 0 \\ 0 & 0 & 0 & 1 \end{bmatrix}.$$

The continuous-state-space Eq.(3) can be rewritten into a discrete-state-space equation for digital control as follows:

$$\begin{aligned} \xi(\kappa+1) &= A_d\xi(\kappa) + B_d u(\kappa) \\ Y_{out}(\kappa) &= C_d\xi(\kappa), \end{aligned} \tag{4}$$

with the matrices $A_d \subseteq \mathbb{R}^{4\times4}$, $B_d \subseteq \mathbb{R}^{4\times2}$, $C_d \subseteq \mathbb{R}^{4\times4}$.

3. Advanced control techniques for active suspension systems

The control system for the active suspension system consists of three main blocks: the controller, the hydraulic actuator, and the controlled object, which is the suspension system model of

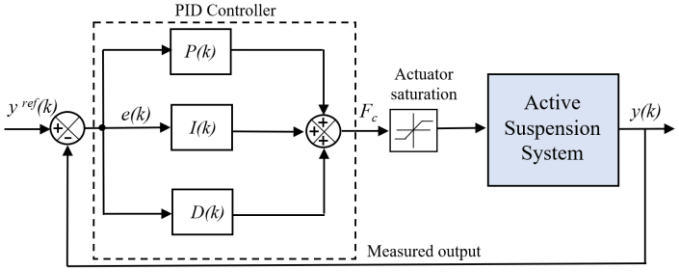

Figure.2. Representative diagram of a PID controller

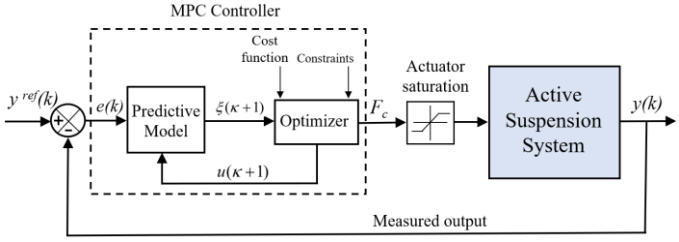

Figure.3. Representative diagram of a MPC controller

the car. The output quantity of interest for the system is the car body oscillation acceleration $a(k)$, while $a^{\text{ref}}(k)$ is the desired output acceleration of the system. To improve the ride comfort of the car, the desired value is $a^{\text{ref}}(k) = 0$, $k = t/T_s$, which means stabilizing the car body acceleration. $e(k)$ is the errorrbetween the output and the desired value of the control system.

$$e(k) = a^{\text{ref}}(k) - a(k). \tag{5}$$

3.1. Design of the PID controller

The PID controller's function is to detect deviations and generate the control signal $F_c(k)$ to ensure the system remains stable while achieving the desired dynamic and static performance. The controller is composed of three control components: proportional (P), integrall (I), anddderivative (D), as expresseddby the following control equation:

$$F_c(\kappa) = \underbrace{K_P e(\kappa)}_{P(\kappa)} + \underbrace{K_I T_s \sum_{i=0}^{k} e(i)}_{I(\kappa)} + \underbrace{K_D \frac{e(\kappa) - e(\kappa-1)}{T_s}}_{D(\kappa)}, \tag{6}$$

where: K_P is the proportional gain, K_I and K_D are the integral and derivative time constants of the PID controller, respectively. The parameters of the PID controller are determined using the second method of Ziegler-Nichols, which involves tuning the controller based on specific system characteristics.

3.2. Design of the MPC controller

The MPC method, as outlined in [14], [15], involves building a model of the actual system to forecast future responses. The

control signal is then computed to minimize the deviation between the predicted future responses and those of the reference model. This approach helps optimize the control system's performance and response, ensuring the system operates accurately and efficiently.

Consider the discrete-state-space model of the system, which includes one input signal and one output signal, as presented in [15]:

$$\begin{cases} \xi_m(\kappa+1) = A_m\xi_m(\kappa) + B_m u(\kappa) \\ Y_{out}(\kappa) = C_m\xi_m(\kappa) \end{cases}, \tag{7}$$

where, $u(\kappa)$ is the control signal, $Y_{out}(\kappa)$ is the output signal, and ξ_m is the state variable. Convert the model to a form that is appropriate for the design objective:

$$\begin{aligned} &\Delta\xi_m(\kappa+1) = \xi_m(\kappa+1) - \xi_m(\kappa) \\ &= A_m(\xi_m(\kappa) - \xi_m(\kappa-1)) + B_m(u(\kappa) - u(\kappa-1)) \\ &= A_m\Delta\xi_m(\kappa) + B_m\Delta u(\kappa). \end{aligned} \tag{8}$$

$$\begin{aligned} &Y_{out}(\kappa+1) - Y_{out}(\kappa) = C_m(\xi_m(\kappa+1) - \xi_m(\kappa)) \\ &= C_m\Delta\xi_m(\kappa+1) \\ &= C_mA_m\Delta\xi_m(\kappa) + C_mB_m\Delta u(\kappa). \end{aligned} \tag{9}$$

Define: $\xi(\kappa) = \begin{bmatrix} \Delta\xi_m(\kappa)^T & Y_{out}(\kappa) \end{bmatrix}^T$

The newly obtained state-space model is as follows:

$$\overbrace{\begin{bmatrix} \Delta\xi_m(\kappa+1) \\ Y_{out}(\kappa+1) \end{bmatrix}}^{\xi(\kappa+1)} = \overbrace{\begin{bmatrix} A_m & 0_m^T \\ C_mA_m & 1_m \end{bmatrix}}^{A_\xi}\xi(\kappa) + \overbrace{\begin{bmatrix} B_m \\ C_mB_m \end{bmatrix}}^{B_u}\Delta u(\kappa),$$

$$Y_{out}(k) = \overbrace{[0_m \quad 1]}^{C_\xi}\begin{bmatrix} \Delta\xi_m(k) \\ Y_{out}(k) \end{bmatrix} = C\xi(k). \tag{10}$$

At the sampling time κ, it is assumed that the state vector $\xi(\kappa)$ has been measured. The set of future control signals is denoted as follows:

$\Delta u(\kappa_i), \Delta u(\kappa_i+1), ..., \Delta u(\kappa_i+N_C-1)$ where N_C is referred to as the control horizon. The components of this control set represent the future control signals. The forecasted state vector is given as: $\xi(\kappa_i+1|\kappa_i), \xi(\kappa_i+2|\kappa_i), ...\xi(\kappa_i+N_p|\kappa_i)$ where N_P is the prediction horizon of the forecast.

Based on the state-space model A_ξ, B_u, C_ξ and the current state vector $\xi(\kappa)$, as well as the set of forecasted control signals $u(\kappa)$, the future state vectors are calculated as follows:

$$\begin{aligned} &\xi(\kappa+1|\kappa) = A_\xi\xi(\kappa) + B_u\Delta u(\kappa), \\ &\xi(\kappa+N_p|k) = A_\xi^{N_P}\xi(\kappa) + A_\xi^{N_P-1}B_u\Delta u(\kappa+1) \\ &+A_\xi^{N_P-2}B_u\Delta u(\kappa+1) + ... + A_\xi^{N_P-N_C}B_u\Delta u(\kappa+N_C-1), \\ &\xi(\kappa+2|\kappa) = A_\xi^2\xi(\kappa) + A_\xi B_u\Delta u(\kappa) + B_u\Delta u(\kappa+1), \end{aligned} \tag{11}$$

The forecasted output variables are calculated as:

$$\begin{aligned} &Y_{out}(\kappa+1|\kappa) = C_\xi A_\xi\xi(\kappa) + C_\xi B_\xi\Delta u(\kappa), \\ &Y_{out}(\kappa+2|\kappa) = C_\xi A_\xi^2\xi(\kappa) + C_\xi A_\xi B_u\Delta u(\kappa) + C_\xi B_u\Delta u(\kappa+1), \\ &Y_{out}(\kappa+N_p|\kappa) = C_\xi A_\xi^{N_P}\xi(\kappa_i) + C_\xi A_\xi^{N_P-1}B_u\Delta u(\kappa+1) \\ &+C_\xi A_\xi^{N_P-2}B_u\Delta u(\kappa+1) + ... + C_\xi A_\xi^{N_P-N_C}B_u\Delta u(\kappa+N_C-1), \end{aligned} \tag{12}$$

Define:

$$\bar{Y} = [Y_{out}(\kappa+1|k)\ Y_{out}(\kappa+2|k) \ldots Y_{out}(\kappa+N_p|\kappa)]^T.$$

Obtained:

$$\bar{Y} = \Gamma\xi(\kappa) + \Upsilon\Delta U, \tag{13}$$

where:

$$\Gamma = \begin{bmatrix} C_\xi A_\xi & C_\xi A_\xi^2 & C_\xi A_\xi^3 & \ldots & C_\xi A_\xi^{N_p} \end{bmatrix}^T,$$

$$\Upsilon = \begin{bmatrix} C_\xi B_u & 0 & 0 & \cdots & 0 \\ C_\xi A_\xi B_u & C_\xi B_u & 0 & \cdots & 0 \\ C_\xi A_\xi^2 B_u & C_\xi A_\xi B_u & C_\xi B_u & \cdots & 0 \\ \vdots & & & & \\ C_\xi A_\xi^{N_p-1}B_u & C_\xi A_\xi^{N_p-2}B_u & C_\xi A_\xi^{N_p-3}B_u & \cdots & C_\xi A_\xi^{N_p-N_C}B_u \end{bmatrix}.$$

For a reference signal $a^{\text{ref}}(t)$ at the sampling time κ, the objective of the control system is to produce a forecasted signal that closely matches the desired reference signal. The signal set within the prediction window is assumed to be non-changing:

$$R_\xi^T = \overbrace{\begin{bmatrix} 1 & 1 & \ldots & 1 \end{bmatrix}}^{N_p} a^{\text{ref}}(\kappa) = \bar{R}a^{\text{ref}}(\kappa), \tag{14}$$

with $\bar{R} = \overbrace{\begin{bmatrix} 1 & 1 & \ldots & 1 \end{bmatrix}}^{N_p}$.

In MPC, the objective function is defined as:

$$J = (R_\xi - \bar{Y})^T\bar{Q}_Y(R_\xi - \bar{Y}) + \Delta U^T\bar{R}_{\Delta U}\Delta U, \tag{15}$$

where $\bar{Q}_Y$, $\bar{R}_{\Delta U}$ denote the weighting matrices specified during controller design. In Eq.(15), the first component aims to reduce the deviation between the predicted output and the desired reference trajectory, while the second component penalizes large variations in the control input ΔU. Thus, the cost function J is formulated to be minimized by balancing tracking accuracy and control effort.

The control input ΔU and the force generated by the actuator are related as follows:

$$\begin{bmatrix} -I \\ I \end{bmatrix} \Delta U(\kappa) = \begin{bmatrix} F_c^{lower} \\ F_c^{upper} \end{bmatrix}. \tag{16}$$

Because the cost function *J* has a quadratic form and the imposed constraints are linear inequalities, the predictive control task can be reformulated as a quadratic programming (QP) problem. Under this formulation, the constrained optimal control problem can be expressed as:

$$\min_{\Delta U} \frac{1}{2} \Delta U^T \bar{H} \Delta U + \bar{F}^T \Delta U, \tag{17}$$

$$\text{subject to } \begin{bmatrix} -I \\ I \end{bmatrix} \Delta U \le \begin{bmatrix} F_c^{lower} \\ F_c^{upper} \end{bmatrix},$$

where, $F^T = 2\left[\Gamma \xi(\kappa) + \bar{R} a^{ref}(\kappa)\right] \bar{Q}_Y \Upsilon$ and $F^T = 2\left[\Upsilon^T \bar{Q}_Y \Upsilon + \bar{R}_{\Delta U}\right]$.

A quadratic problem and leads to a nonlinear solution which can be easily solved by the QP problem in Matlab.

The controller parameters, such as N_P, N_C, R have been chosen to obtain a feedback response with good performance. Thus, the steps to solve the predictive control problem are as follows: Assume that at time k, the values of $\xi_m(\kappa)$ and $u(\kappa)$ are known.

Step 1: *Initialization*: The predictive controller for the active suspension system is designed using the following parameters: $N_P = 10$, $N_C = 5$, $\bar{R}_{\Delta U} = 0.02$, $\bar{Q}_Y = 1$. Calculate $\xi_m(\kappa+1)$ using Eq.(7). This gives:

$$\Delta\xi_m(\kappa+1) = \xi_m(\kappa+1) - \xi_m(\kappa), \quad Y_{out}(\kappa+1) = C_m \xi_m(\kappa+1).$$

Step 2: *Calculate:*

$$\xi(\kappa+1) = \begin{bmatrix} \Delta\xi_m(\kappa+1) \\ Y_{out}(\kappa+1) \end{bmatrix}.$$

Step 3: *Optimization*: solve the optimal control problem $\min_{\Delta U} \frac{1}{2} \Delta U^T \bar{H} \Delta U + \bar{F}^T \Delta U$ with *J* from (15) subject to (16).

Step 4: *Implementation*: Determine the variation of the control value $\Delta U(\kappa+1)$ as the first element of ΔU.

Therefore, the control signal at step $\kappa+1$ is

$$u(\kappa+1) = u(\kappa) + \Delta u(\kappa+1).$$

Then, we proceed with calculating the state vector $\xi_m(\kappa+1)$ at the next sampling time $\kappa+1$. Update and go to step 1.

4 Results and analysis

This study utilizes numerical simulation techniques to evaluate the performance of two controllers, PID and MPC, for the active suspension system in the time domain. The simulation is driven by excitation from road surface irregularities, the primary source of vibration. The author examines the suspension system's oscillation as the car moves over two commonly encountered road profiles: a sine wave with a frequency of 10(rad/s) and an amplitude of 0.07(m), and a step wave with a bump height of 0.035(m).

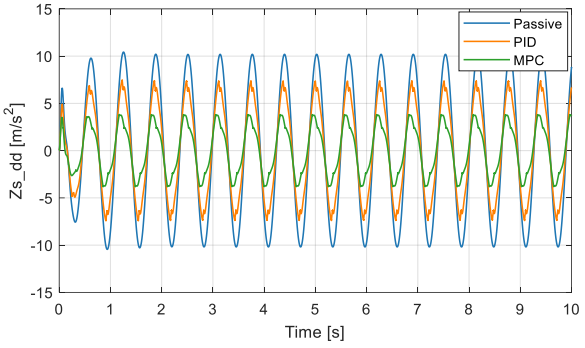

Figure.4. Comparison of active suspension body acceleration based on the sin road profile.

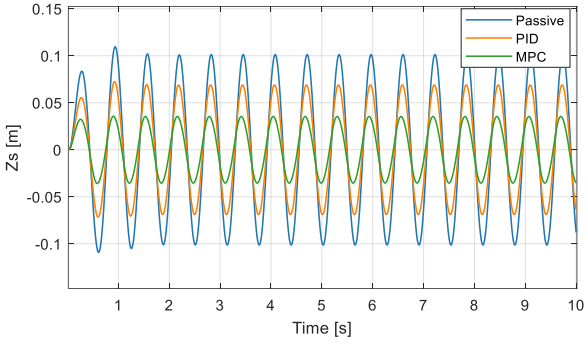

Figure.5. Comparison of active suspension body displacement based on the sin road profile.

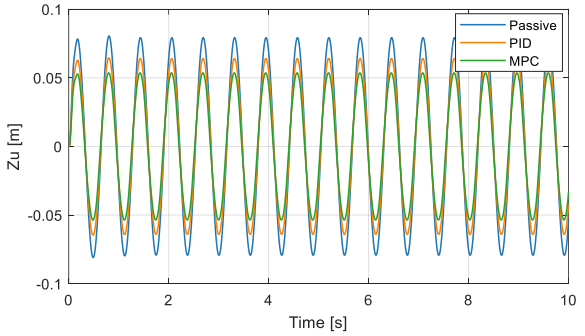

Figure.6. Comparison of sprung-mass displacement based on the sin road profile.

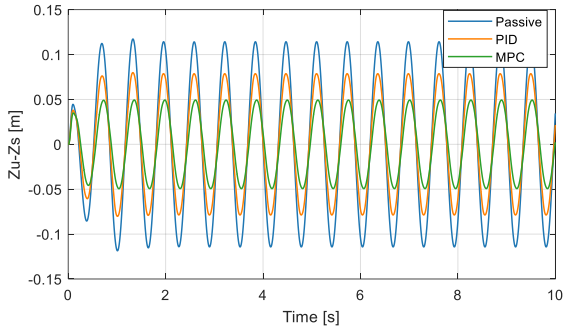

Figure.7. Comparison of suspension deflection based on the sin road profile.

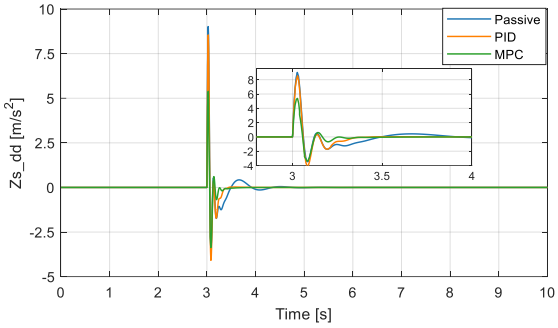

Figure.8. Comparison of active suspension body acceleration based on the step road profile.

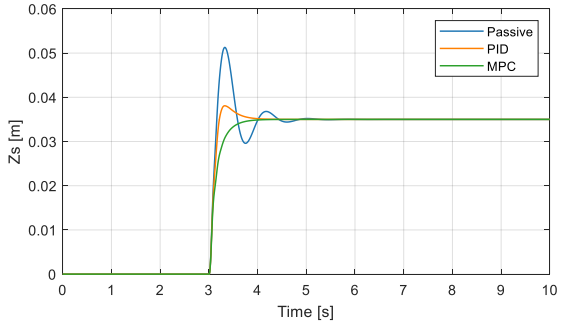

Figure.9. Comparison of active suspension body displacement based on the step road profile.

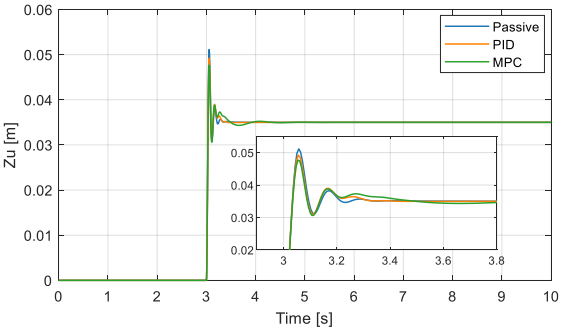

Figure.10. Comparison of sprung-mass displacement based on the step road profile.

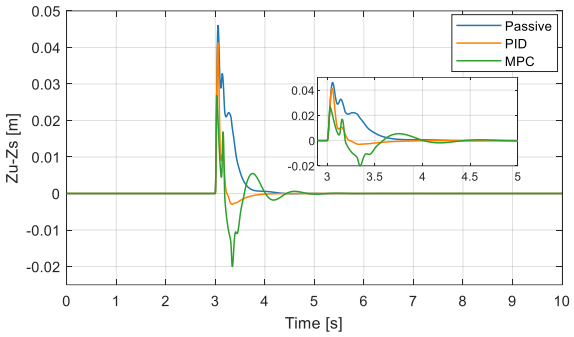

Figure.11. Comparison of suspension deflection based on the step road profile.

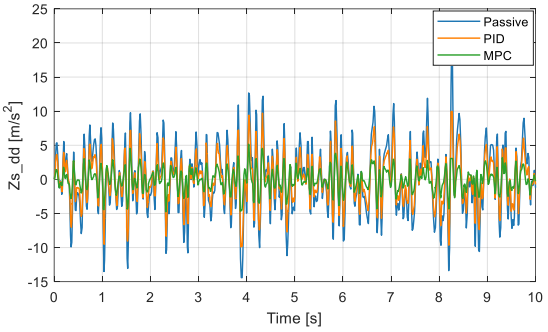

Figure.12. Comparison of active suspension body acceleration based on the random road profile.

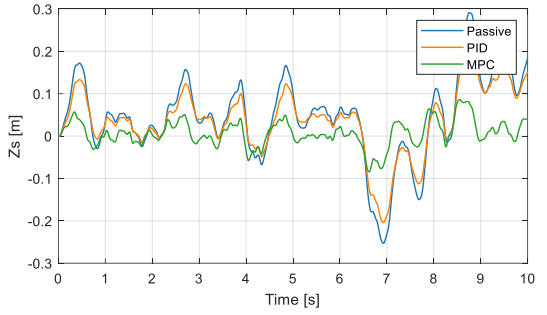

Figure.13. Comparison of active suspension body displacement based on the random road profile.

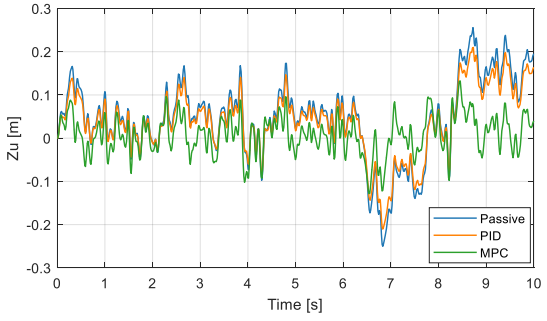

Figure.14. Comparison of sprung-mass displacement based on the random road profile.

Table 1. Evaluation of the ride comfort improvement

Control method	Body aceleration (Max. value)	Acceleration RMS (m/s^2)	Comfort level
Sin road profile			
Passive	7.682 (m/s^2)	2.251	Very bad
PID	6.308 (m/s^2)	1.362	Bad
MPC	3.750 (m/s^2)	0.523	Good
Step road profile			
Passive	7.0159 (m/s^2)	1.590	Bad
PID	5.7443 (m/s^2)	0.781	Mean
MPC	3.3884 (m/s^2)	0.342	Good
Random road profile			
Passive	17.204 (m/s^2)	2.367	Very bad
PID	9.9466 (m/s^2)	1.152	Bad
MPC	5.1582 (m/s^2)	0.332	Good

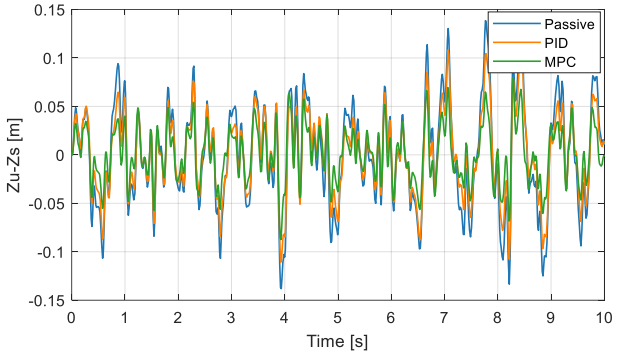

Figure.15. Comparison of suspension deflection based on the random road profile.

The output includes values related to ride comfort (body acceleration), displacement, and suspension travel.

Figures 4-7, 8-11 and 12-15 display the simulation results for body acceleration, body displacement, axle displacement, and un-sprung displacement of the suspension system in response to the sine road profile, the step road profile, and the random road profile. The body and axle displacements under road surface excitation are described in Figures 5, 6; Figures 9, 10; Figures 13, 14. The results indicate that the displace-ment values for the car with a passive suspension system are significantly higher compared to those with an active suspension system. For the passive suspension system, the maximum body displacement is 0.076(m); 0.0513(m); 0.2914(m) for the sine road profile, the step road profile, and the random road profile respectively. In contrast, for the active suspension system using the PID controller, the maximum displacements are 0.06m; 0.037(m); 0.2295(m). As in figure results, for the active suspension system, the body displacement using the PID controller is larger than that using the MPC controller. The use of the MPC-controlled active suspension system leads to a substantial improvement in car body displacement.

Body acceleration is a crucial parameter for assessing a car's ride comfort during vibration. The acceleration of body displacement is directly proportional to the body displace-ment when the road profile changes. Similar to displacement, the maximum body acceleration values are 7.682(m/s^2); 7.0159(m/s^2); 17.204(m/s^2) for the passive suspension system; 6.308(m/s^2); 5.7443(m/s^2); 9.9466(m/s^2) for the active suspension system using the PID controller; and 3.750(m/s^2); 3.3884(m/s^2); 5.1582(m/s^2) for the active suspension system using the MPC controller.

As shown in Figures 7, 11 and 15, the suspension travel in both the PID and MPC systems is progressively reduced compared to the passive suspension system. This reduction helps lower the car's center of gravity, thereby improving its stability and ensuring better grip with the road. The active suspension system using the MPC algorithm can be effectively implemented and operate in a confined space. By utilizing the MPC control algorithm, the car's oscillations are more effectively controlled, resulting in improved comfort for passengers. The sim-

ulation results demonstrate that the MPC controller not only significantly enhances the control of car body oscillations but also optimizes the suspension travel, keeping it within the design safety limits. Furthermore, by minimizing the body acceleration, MPC provides superior comfort and stability compared to traditional control methods, such as PID.

To better demonstrate the effectiveness of the proposed control strategy, assessing comfort only through the acceleration limit approach is insufficient, as it does not fully reflect the suspension's performance during the entire ride. Consequently, in accordance with the ISO 2631 standard [17], the Root Mean Square (RMS) acceleration method is adopted, which determines the mean acceleration over a specified time interval.

The expression for the weighted RMS acceleration is defined as:

$$\ddot{z}_{s,RMS} = \left[\frac{1}{T} \int_0^T \ddot{z}_{s,RMS}^2(t) dt \right]^{0.5}, \quad (18)$$

where, $\ddot{z}_{s,RMS}(t)$ represents the weighted acceleration, while T refers to the measurement duration.

The ISO 2631 standard, e.g (see in [18]) specifies comfort level values that serve as approximate indicators of ride comfort in public transportation. Based on these reference values, Table 1 provides a quantitative evaluation of the improvement in ride comfort. Table 1 demonstrates that the maximum value deviations for acceleration of body displacement and RMS value in the MPC controller are smaller than those observed in both the PID controller and the passive suspension system. It can thus be concluded that the MPC controller proposed in this study represents an effective approach for active suspension control, particularly in the context of high-end vehicles.

The PID controller is generally suited for straightforward applications requiring fast response and stability, whereas MPC is more appropriate for complex systems that necessitate precise prediction and flexible control actions. The presented method yields a notable reduction in body acceleration, which contributes to greater stability and improved tire–road contact.

5 Conclusion

In this paper, the author has developed controllers for the active suspension system of a quarter-car model using PID and MPC control methods, with the primary goal of improving the car's ride comfort. The simulation results show that the implementation of an active suspension system offers substantial advantages over the traditional passive suspension system.

The simulation results indicate that the MPC controller significantly lowers the body acceleration amplitude compared to both the PID controller and the passive suspension system. This reduction in body acceleration leads to a substantial decrease in vibrations, thereby enhancing ride comfort and overall driving experience.

The suspension travel under MPC control is considerably reduced compared to both the PID and passive systems, highlighting its effectiveness in maintaining system stability. Given these simulation results, the implementation of the MPC controller for a fully functional active suspension system is a practical and viable solution for cars.

Acknowledgment

This research is funded by Funds for Science and Technology Development of the University of Danang under project number B2024-DN02-22.

Conflict of Interest Statement

The authors declared no potential conflicts of interest with respect to the research, authorship, and/or publication of this work.

CRediT Author Statement

Duc Lich Luu: Methodolog, Conceptualization, Validation; Formal analysis,Writing – review and editing; **Nguyen Quang Trung**: – review and editing; **Ngoc Thien To**: Methodolog, Formal analysis. All authors have read and agreed to the published version of the manuscript.

References

[1] Zhu S, Xu G, Tkachev A, Wang L, Zhang N. Comparison of the road-holding abilities of a roll-plane hydraulically interconnected suspension system and an anti-roll bar system. Proc Inst Mech Eng D J Automob Eng. 2017;231(11):1540-1557. https://doi.org/10.1177/0954407016675995

[2] Gao J, Han P. Research on optimal matching of vehicle suspension parameters for improving vehicle ride comfort on bump road. Adv Mech Eng. 2023;15(5):16878132231175751. https://doi.org/10.1177/16878132231175751

[3] Qin Y, Wei C, Tang X, Zhang N, Dong M, Hu C. A novel nonlinear road profile classification approach for controllable suspension system: Simulation and experimental validation. Mech Syst Signal Process. 2019;125:79–98. https://doi.org/10.1016/j.ymssp.2018.07.015

[4] Çelik İ, Arslan T A, Aysal F E, Bayrakçeken H, Oğuz Y, Comparison of Control Methods for Half-Car Active Suspension System. International Journal of Automotive Science And Technology. 2024; 8(4):439-450. https://doi.org/10.30939/ijastech..1578123

[5] Baráth B. The Effect of Poor Road Surfaces on Vehicle Suspension Geometry and the Misalignment of Setup Parameters. International Journal of Automotive Science And Technology, Special Issue 1st Future of Vehicles: Innovation, Engineering and Economic Conference. 2025; 9:28-34. https://doi.org/10.30939/ijastech..1766086

[6] Sistla P, Chemmangat K, Figarado S. Design and implementation of passivity-based controller for active suspension system using

port-Hamiltonian observer. Proceedings of the Institution of Mechanical Engineers, Part D: Journal of Automobile Engineering. 2023; 237(14): 3367-3379 . https://doi.org/10.1177/09544070221147364

[7] Yatak M. Ö, Hisar Ç, Şahin F. Fuzzy Logic Controller for Half Vehicle Active Suspension System: An Assessment on Ride Comfort and Road Holding. International Journal of Automotive Science And Technology. 2024; 8(2):179-187. https://doi.org/10.30939/ijastech..1372001

[8] Souilem H, Mehjoub S, Derbel N. Intelligent control for a half-car active suspension by self tunable fuzzy inference system. Int J Fuzzy Syst Adv Appl. 2015;2:9–15.

[9] Boulaaras Z, Aouiche A, Chafaa K. Intelligent FOPID and LQR Control for Adaptive a Quarter Vehicle Suspension System. European Journal of Electrical Engineering. 2023;25(1-6):1-8. https://doi.org/10.18280/ejee.251-601

[10] Bai R, Wang H B. Robust optimal control for the vehicle suspension system with uncertainties. IEEE transactions on cybernetics. 2021; 52(9):9263-9273. https://doi.org/10.1109/TCYB.2021.3052816

[11] Koch G, Kloiber T. Driving state adaptive control of an active vehicle suspension system. IEEE Trans Control Syst Technol. 2014;22:44–57. https://doi.org/10.1109/TCST.2013.2240455

[12] Lauwerys C, Swevers J, Sas P. Robust linear control of an active suspension on a quarter car testrig. Control Eng Pract. 2005;13:577–86. https://doi.org/10.1016/j.conengprac.2004.04.018

[13] Li P, Lam J, Cheung KC. Multi-objective control for active vehicle suspension with wheelbase preview. J Sound Vib. 2014;333:5269–82. https://doi.org/10.1016/j.jsv.2014.06.017

[14] Luu DL, Pham HT, Lupu C, Nguyen TB, Ha ST. Research on cooperative adaptive cruise control system for autonomous vehicles based on distributed model predictive control. In: 2021 International Conference on System Science and Engineering (ICSSE); 2021. p. 13–8. https://doi.org/10.1109/ICSSE52999.2021.9538410

[15] Wang L. Model predictive control system design and implementation using MATLAB. Vol. 3. London: Springer; 2009.

[16] Munawwarah S, Yakub F. Control analysis of vehicle ride comfort through integrated control devices on the quarter and half car active suspension systems. Proceedings of the Institution of Mechanical Engineers, Part D: Journal of Automobile Engineering. 2021; 235(5):1256-1268. https://doi.org/10.1177/09544070209683

[17] BS ISO 2631-5:2018. Mechanical vibration and shock evaluation of human exposure to whole-body vibration. International Standard. ISO, 2018.

[18] Dridi, I, Hamza, A, Ben Yahia, N. A new approach to controlling an active suspension system based on reinforcement learning. Advances in Mechanical Engineering, 2023; 15(6): 16878132231180480. https://doi.org/10.1177/16878132231180480